

ENHANCEMENT OF WEAR RESISTANCE AND HARDNESS OF THE H13 TOOL STEEL BY USING TUNGSTEN CARBIDE COATING

Hamdi Abdulhamid Raghs

Faculty of Engineering, Omar Al Mukhtar University, Libya

hamdi.raghs@omu.edu.ly

المخلص

في هذا البحث ، تم دراسة تأثير طلاء كربيد التنجستن على الأداء التريبولوجي لصلب H13 من خلال إجراء اختبارات التآكل ، وقمنا بإجراء تحليل لطلاء كربيد التنجستن على أداء التآكل لصلب H13 بتقنية بصرية باستخدام مجهر المسح الإلكتروني (SEM) وصور طبوغرافية ثنائية الأبعاد وثلاثية الأبعاد وكذلك تجربة معامل الاحتكاك ومعلمات فقدان الحجم. وفقاً للنتائج التي تم الحصول عليها من اختبارات التآكل ، قلل الفولاذ المطلي بكربيد التنجستن معامل الاحتكاك بنسبة 23 ٪ مقارنة بالفولاذ غير المطلي ، وكانت آلية التآكل أكثر سطحية. الهدف من هذه الدراسة هو زيادة مقاومة التآكل والصلابة لفولاذ العمل الساخن H13 باستخدام طلاء كربيد التنجستن.

Abstract

In this research, study the effect of coating of tungsten carbide on tribological performance of H13 tool steel was investigated by wear tests, and we made analysis for tungsten carbide coating on wear performance of H13 steel with visually technique by using Scanning Electron Microscope (SEM) and 2D-3D topography images, friction coefficient experiment, and volume loss parameters. As per the results which obtained from wear tests, the tungsten carbide coated steel decreased the friction coefficient by 23% compared to the uncoated steel, and a mechanism of wear was more superficial. The aim of this study is to increase the wear resistance and hardness of H13 hot work tool steel by using tungsten carbide coating.

Keywords: Five keywords, WC coating, H13 tool steel, High Velocity Oxygen Fuel (HVOF), wear resistance, hardness, tungsten carbide coating

1. Introduction

As a result of the increase in the properties expected from the materials used in engineering fields and the advancement of technology, the need for long-lasting, high-performance and low-cost new engineering materials has arisen. As a result of problems in meeting this need with existing materials, a field known as surface engineering has emerged. In surface engineering, studies are carried out on the development, structure, production and use of a material's physical or chemical properties, from the bottom surface of a material to the interface, from the interface to the coating [1,2,3,4].

H13 hot work tool steels are exposed to high wear and surface deformation due to working conditions. For this reason, it is important to coat H13 steels and to protect surface forms with coatings that can be used in the working environment. Hot work tool steels are used for industrial applications at temperatures of 200 °C and above. These tool steels containing Cr, Mo, V alloying elements have high hardness and toughness. H13 tool steels are generally used as materials for hot extrusion, hot pressing, casting and molding [5, 6, 7, 8].

This steel are exposed to stresses such as fatigue, creep, plastic deformation, thermal forces and wear, depending on the temperature of the environment in which they are used. For this reason, micro-macro cracks and deformities occur on the material surface. In order to minimize these deformations, various surface hardening methods are used. In industrial applications, surface hardening methods such as cementation, nitriding, carburizing is used, as well as coating process [9, 10, 11, 12].

2. Material and methods

H13 tool steel was used in the experiments and its chemical components are given in Table 1. H13 tool steel was preferred in the study because it is the most widely used in hot work and it exhibits superior tribological performance compared to other steels.

For this reason, within the scope of the study, the wear resistance of H13 steel was tried to be increased with WC-Co coating. It is foreseen that the results obtained will also be a reference for other hot work steels, and wear tests were carried out, before the coating process and wear tests, the sample surfaces were cleaned using sandpaper papers numbered 200-400-800-1000 in order to remove the oxide layer on the surface.

Table 1: Chemical composition of AISI H13 hot work steel

| Chemical Composition (%) | C | Cr | Mn | Si | Ni | Mn |
|--------------------------|-----|-----|-----|-----|-----|-----|
| | .40 | .30 | .50 | .20 | .10 | 0.4 |
| | | | | | | 5 |



Fig. 1 AISI H13 steel samples

Wear samples were prepared in dimensions of 30 mm x 10 mm x 5 mm. To increase the tribological performance of H13 steel and samples of H13 was covered with tungsten carbide material. Tungsten carbide is widely used especially in industrial applications subject to shear wear, as it increases the hardness of the materials as well as the wear and corrosion resistance.

Due to the high mechanical and tribological properties of tungsten carbide (WC) material, tungsten carbide was preferred as the coating material for the minimization of wear and corrosion-induced deformations on the steel surface. Cobalt (Co) was used as the binder material to ensure adequate adhesion between tungsten carbide and H13 steel. Cobalt can interact well with elements of carbides group and provide high wettability and solubility performance on the surface.

Thanks to the ductile Co reinforced to the tungsten carbide material, a coating layer with high fracture toughness, hardness and corrosion resistance is formed on the surface. The reinforcement ratio of the binder material is also important for the coating to provide the desired tribological performance. As the amount of cobalt increases, the porosity decreases and the cohesive force between the coating and the base material increases.

In addition, as the amount of cobalt increases, the hardness increases, but after a certain rate, the increase in the amount of cobalt decreases the thermal fatigue resistance of the material depending on the hardness and strength. This situation adversely affects the mechanical properties of the material.

In the study, we analyzed the tribological performance of cobalt (Co) reinforced tungsten carbide (WC) coatings with hardness measurement, cumulative mass loss measurement, friction coefficient values and investigated the effect of Co ratio on friction and wear resistance.

In addition, the coating processes performed with High Velocity Oxygen Fuel (HVOF) provide low porosity, high toughness and corrosion resistance properties, as well as providing the opportunity to obtain ceramic coatings with high hardness, strength and wear resistance thanks to the residual compressive stress they create. The fact that it can be carried out at low cost and that it does not have negative ecological effects are also important factors that increase its use in industrial applications.

In the present study, the HVOF method was preferred considering tribological and mechanical performance, economic and environmental factors. The microhardness values of the samples were measured with Bruker UMT Universal hardness measuring device and the obtained values are given in Table 2. The hardness values were calculated by taking the average after six measurements were made.

Table 2: Hardness values of samples

| Sample Type | Hardness Value (Vickers) |
|---------------------|--------------------------|
| Pure Sample | 261 ± 40 HV |
| WC-Co Coated Sample | 1075 ± 110 HV |

A roller-on-plate type tribometer was used in the experiments. Experiment parameters and photographs of the wear bench are shown in Table 2 and Figure 2. In the roller on plate system, the abrasive ball is released to make a rolling motion and the steel friction is tried to be simulated

. Experiments were carried out in pure water environment to simulate dry and atmospheric conditions. The ambient temperature of the experiment and the pure water temperature used in the experiments are ~23°C. In the measurements made during the experiments, it was determined that the ambient and water temperature changed at a negligible level. The volume of pure water in which the experiments were carried out was 300 ml. As abrasive material in the test system; A 100Cr6 steel ball with a hardness of 50 HRC was used.

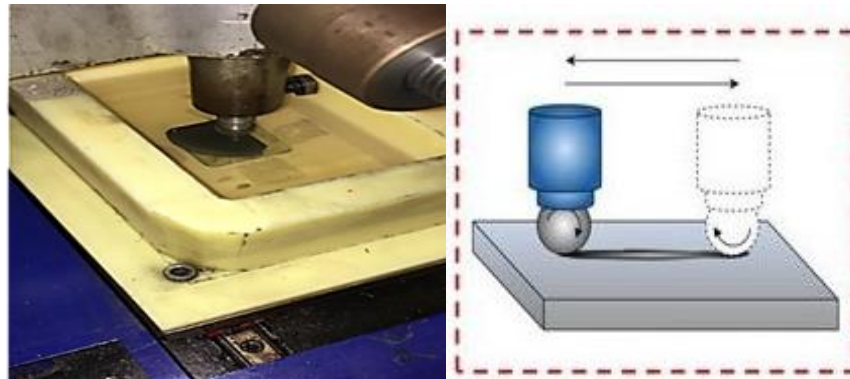


Fig. 2 Photograph of the wear bench

SEM imaging, elemental analysis (EDX) and microhardness measurement methods were used for the characterization of the coated samples. Linear method and mapping method were used in EDX analysis. A dynamometer with an accuracy of ± 0.1 N was used to measure the friction coefficient. SEM, EDX and 3D topography (Phase View Optical Profilometer) imaging methods were used for surface morphology analysis.

For the quantitative analysis of the deformations on the surface, the width (a) and depth (b) values of the wear trace were determined from the wear profile images obtained with a 2D profilometer, and the stroke distance (c) was measured with the help of a caliper (Figure 3). Using the obtained width, depth and stroke distance values, the wear volume values were calculated with the help of the equation given in Eq.1.

$$V = \frac{2}{3} a \cdot b \cdot c \dots \dots \dots (1)$$

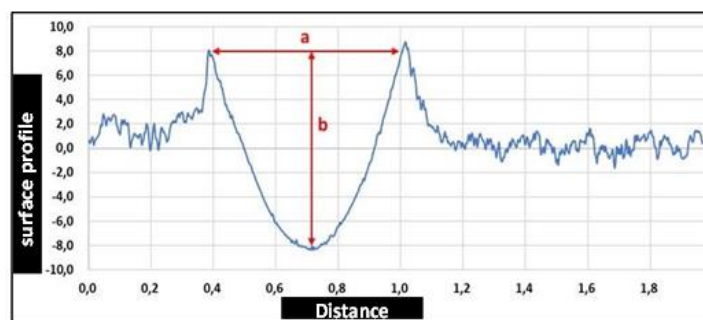


Fig. 3 Example of wear profile obtained with a 2D profilometer

3. Experimental Results and Discussion

The results were analyzed in two stages, metallurgical and tribological characterization of WC-Co coated samples. Hardness measurement and SEM, XRD, EDX (line and mapping) images were analyzed in metallurgical characterization. In the tribological characterization, the friction coefficient values obtained during the wear tests and the volume loss values after the wear were analyzed; in addition, the surface morphology was examined with SEM and 3D topography images.

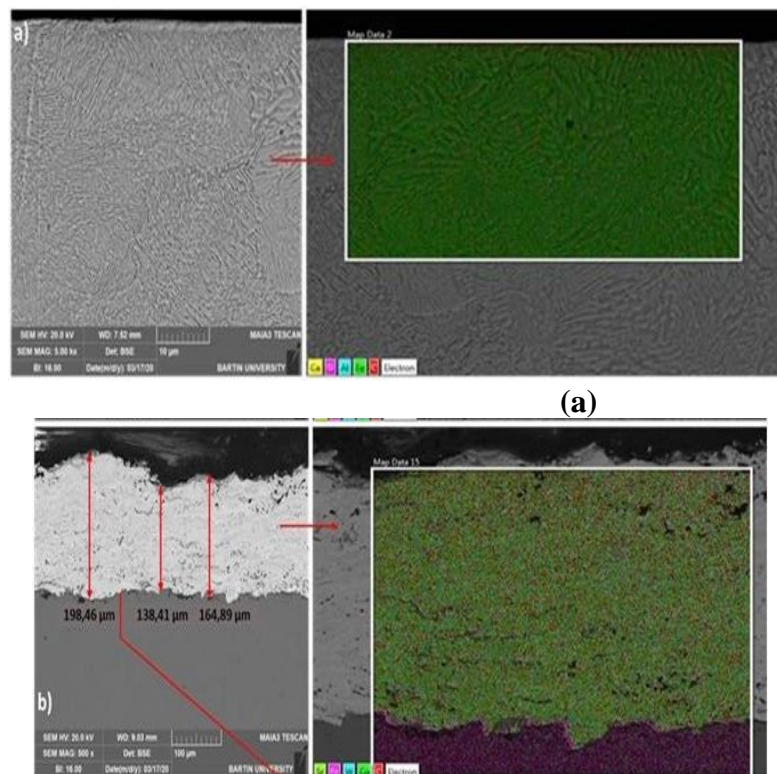
3.1. Characterization of Tungsten Carbide (WC) coating layer:

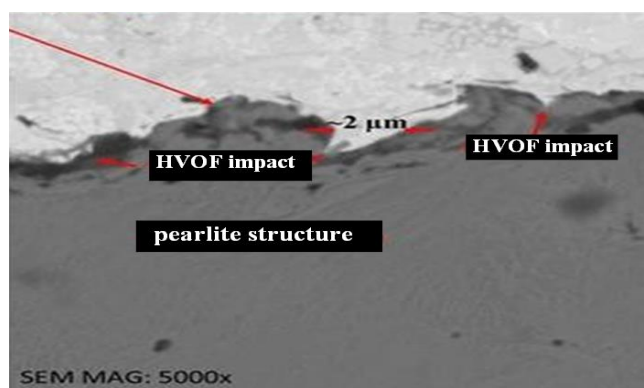
Carbide-based coatings draw attention in the development of the surface properties of engineering materials. Intermediate solid solutions formed thanks to the atomic radius of ~0.071 nm of carbon can increase the tribological performance of materials subject to wear with their high hardness properties [13,14].

Depending on the stability of the coating process, homogeneous coating thicknesses can be obtained. The cross-sectional view of WC-12%Co material coated with HVOF on H13 steel is given in Figure 4.

Figure 4.a shows the pearlite microstructure, and Figure 4.b shows an average of 165 µm tungsten carbide (WC) coated cross section over the pearlite structure. It is seen that the coating forms a wavy surface form due to its high thickness. It has been observed in the literature that similar forms occur on WC-coated surfaces [15,16]. It can be said that a wavy form is formed on the surface depending on the spray rate of the HVOF method. The high spray rate in the HVOF method has made the surface form wavy by making a ball forging effect. However, fine-grained structure formation seen in ball forging processes was not observed in the internal structure

Due to the short HVOF treatment time and the formation of a tungsten carbide (WC) layer on the surface during the process, no microstructure change occurred. According to the SEM image, it was determined that the minimum amount of cracks, voids and tear defects occurred in the coating layer. Considering the thickness of the coating layer, it can be claimed that the resulting defects are negligible. In Figure 4.b, homogeneously dispersed tungsten carbide (WC) particles are seen in the 12% cobalt matrix. Although tungsten carbide (WC) particles have a high tendency to agglomerate, it can be seen from the elemental mapping image that a homogeneous distribution is achieved thanks to the cobalt binder.



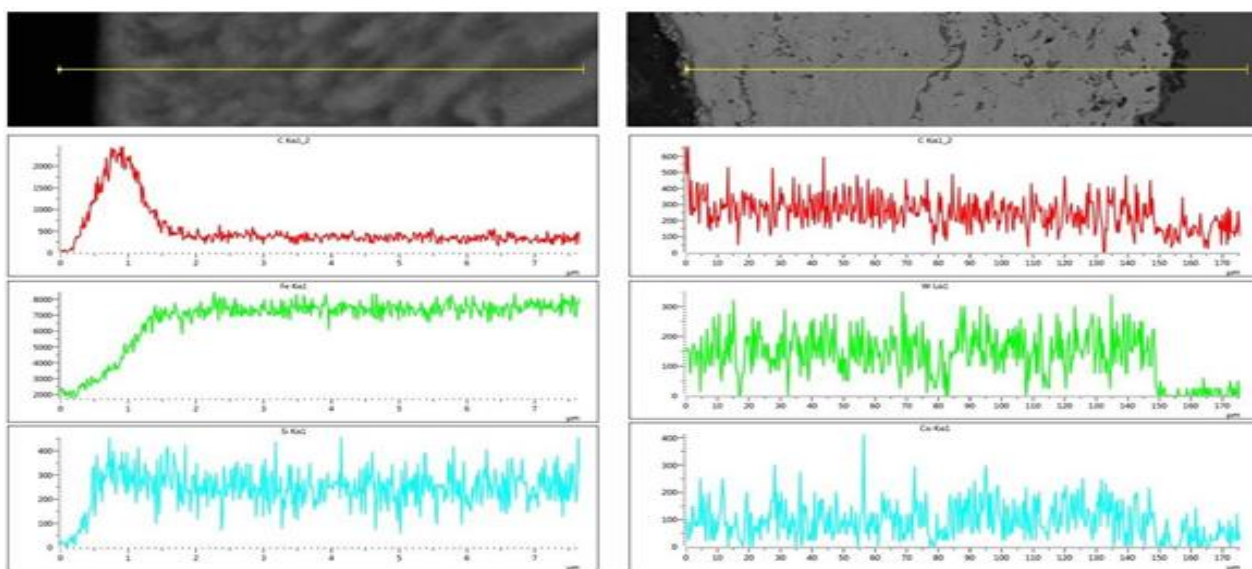


(b)

Fig. 4 a) SEM image of the surface cross -section of the pure sample, b) SEM image of the surface section of the coated sample

EDX analyses for analysis of coating quality are given in Figure 5. In Figure 5.A, the surface of the unlocked sample was seen on the surface of the oxide layer. After the coating process, it is seen that the carbon distribution is homogeneous on H13 steel material surface. It can be said that the oxide layer is dispersed depending on the pressure and temperature in the coating process and with the effect of decay.

The dominant elements (C, W, Co) seen in Figure 5.b are homogeneously along the coating layer. Depending on this situation, it can be claimed that the coating is of sufficient quality in terms of spectral.



(a)

(b)

Fig. 5 a) EDX analysis of the surface of the pure sample, b) EDX analysis of the surface of the coated sample

In addition to the elemental homogeneity of the coating, the bond formed with base material is also important. It is seen in the XRD graph in Figure 6 where the Fe₃W₃C alloy occurs

due to the solid state solution formed with base material. It can be argued that a stable bond formation occurs thanks to the cubic crystal cage structure of the alloy. The formation of WC and W₂C peaks seen in Figure 6 is expected for Tungsten -coated alloys.

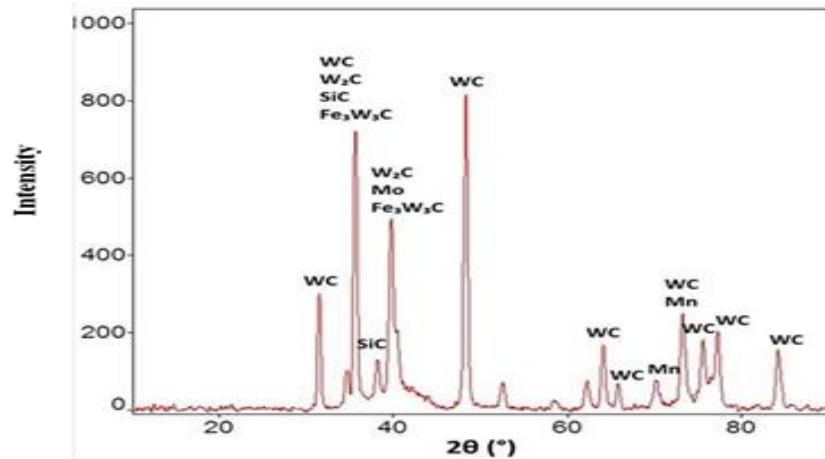


Fig. 6 XRD analysis

In Figure 4 and Figure 5, it is seen that there is no color change or tone difference for WC and W₂C. However, according to the graph given in Figure 7, it is observed that WC layer of ~ 750 HV stiffer occurs on the material surface, and then W₂C layer, which reaches a maximum of 1250 HV hardness due to oxidation.

While there was no change in hardness along WC layer, the hardness value of the W₂C layer increased first and then decreased. It can be said that variability occurs in the hardness layer due to oxidation rate and HVOF parameters. Another remarkable situation in the hardness graph is that the transition zone is at a distance of ~ 50 μm. In this region, the hardness value decreased in a controlled manner, forming a linear trend from 750 HV to 250 HV. This trend can be evaluated as a positive situation in terms of coating strength. Thanks to the controlled drop, stress concentrations that may occur due to hardness changes during the force flow in the material will be minimized and the service life of the coating layer will be extended.

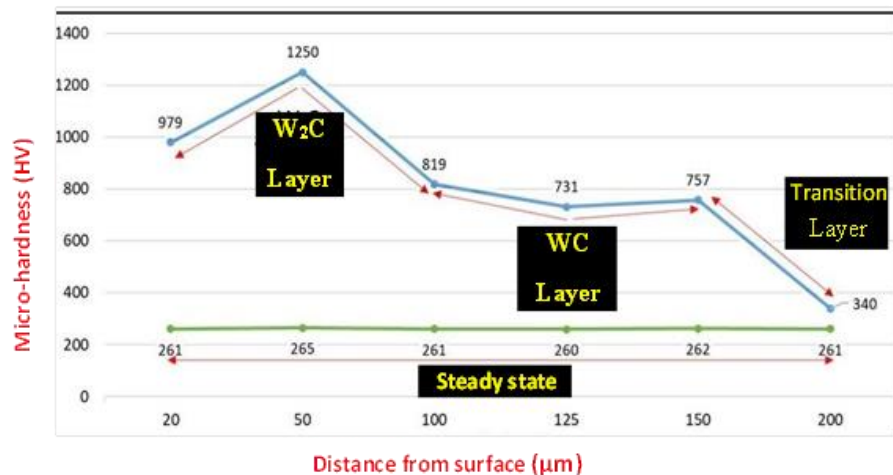


Fig. 7 Microhardness graph

3.2. Tribological performance of tungsten carbide (wc) layer in dry and pure water conditions:

For the tribological performance analysis, firstly, the friction coefficient data were examined. According to Figure 8, the friction coefficient of the uncoated H13 steel sample in the pure water environment decreased by 23% compared to the dry environment. This can be explained by the film layer formed by pure water in the roughness region at the abrasion interface. The compressive and shear stresses formed during friction with the film layer decreased and the friction coefficient decreased.

The decrease in the friction coefficient is not meaningful in terms of the scope of the study, considering the fact that the rails do not have the possibility to work in a continuous water environment and the negative effect of the water environment in terms of braking is taken into account. However, the values obtained in the aquatic environment are important to analyze the effect of the coating. It has been determined that the friction coefficient value of the tungsten carbide (WC) coated sample is the same as the friction coefficient value of the uncoated sample in pure water environment. This shows that ~750 HV hardness increase creates a liquid film layer effect. The hardness of the coating increased from 260 HV to an average of 1000 HV, resulting in a 23% lower friction coefficient. The decrease in the friction coefficient indicates that the tungsten carbide (WC) coating is effective and applicable to reduce the amount of friction on the steel.

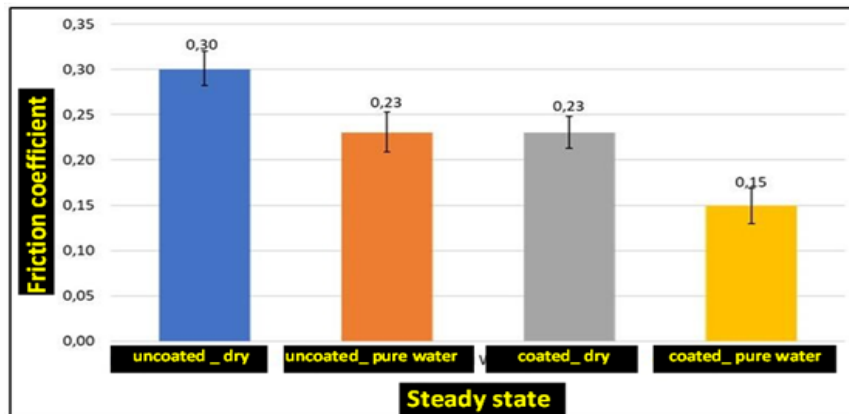


Fig. 8 Friction coefficient values

The decrease in friction coefficient as a result of tungsten carbide (WC) coating is not significant in terms of adherence between H13 steel and other metals, for example sliding process. The adherence value, which expresses the ability of metals to hold onto the steel, is expected to decrease with the decrease in the friction coefficient. For this reason, tungsten carbide (WC) coating cannot be applied in all industrial applications due to technical and economic requirements. However, tungsten carbide (WC) coating can be applied on sliding friction rather than rolling friction occurs. In these regions, reducing the friction coefficient with tungsten carbide (WC) coating is important in terms of minimizing deformations.

Tungsten carbide (WC) coating has a hexagonal tight-packed structure (hsp), while steel has a volume-centered cubic (hmk) crystal lattice structure. Especially under pressure and temperature, that is, in environments with high energy input to the material, the bond formation between hsp and hmk structures accelerates. It can be argued that as a result of the constant contact of H13 steel and other metals,, the bond strength between the coating and the steel will increase

due to the increased pressure and temperature as a result of friction. Increasing temperature and pressure in the tungsten carbide (WC) coated areas where sliding friction occurs can increase the bond strength of the tungsten carbide (WC) coating, making an additional contribution to the wear resistance. In this way, the secondary wear times of engineering materials will increase. Reducing the friction coefficient with tungsten carbide (WC) coating in areas where steel deformation is intense and extending the secondary wear time of the coating thanks to the energy input during the high friction are significant in terms of increasing the useful life of the steel. However, in the long term, the coating thickness will decrease depending on the deformations on the coating surface.

The roughness images obtained with the 2D profilometer for wear volume analysis are given in Figure 9.

While a significant wear pit formation was observed in the uncoated samples, it was observed that no obvious wear traces were formed in the tungsten carbide (WC) coated samples. However, it was determined that the wear trace depth in the coated samples progressed up to 15 μm in dry and pure water environments (Figure 9.c and Figure 9.d). Considering the average coating thickness of $\sim 150 \mu\text{m}$, it is seen that 10% wear depth occurs.

It can be claimed that deformation occurs in the form of brittle fracture due to the extreme hardness on the surface of the coated samples and the depth reaches 15 μm due to crack propagation. After this depth, it can be accepted that the high hardness values formed by W₂C begin and crack propagation stops (Figure 7). On the other hand, the wear widths in the coated samples are at a minimum level compared to the uncoated samples. This indicates that the abrasive ball can penetrate the coating at a superficial level. However, as mentioned above, the capillary cracks formed by the pressure effect in the hard layer advanced into the depths of the material under repeated load. This effect is negligible when the total coating thickness is taken into account. Uniform wear forms in the uncoated samples suggest that the abrasive material eroded the steel material in an abrasive form (Figure 9.a and Figure 9.b). The resulting form is expected when comparing the hardness of the steel (260 HV) with the hardness of the abrasive ball (505 HV). The roughnesses that occur in the wear profile line in Figure 9.b can be expressed as the points where the water film is interrupted by the pressure effect (semi-fluid friction state).

According to Figure 9.c and d, the wear mechanism occurring in the coated samples can be defined as rapid fatigue wear. Depending on the hardness, cracks formed under cyclic loading progressed very quickly. Although this situation seems to be a catastrophic deformation state, no problem has arisen in terms of the reliability of the coating thanks to the mechanisms that stop the crack propagation in the substrate.

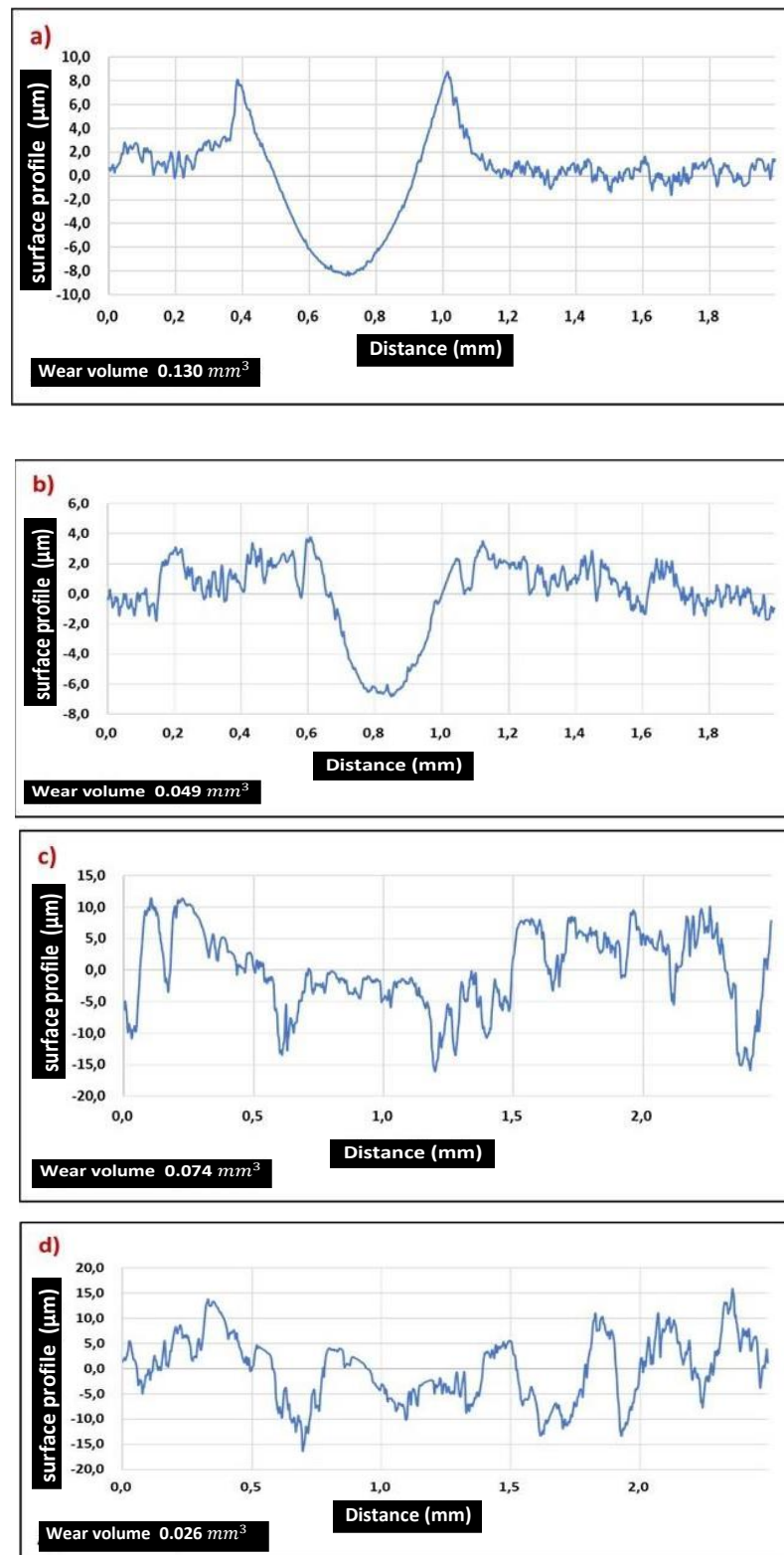
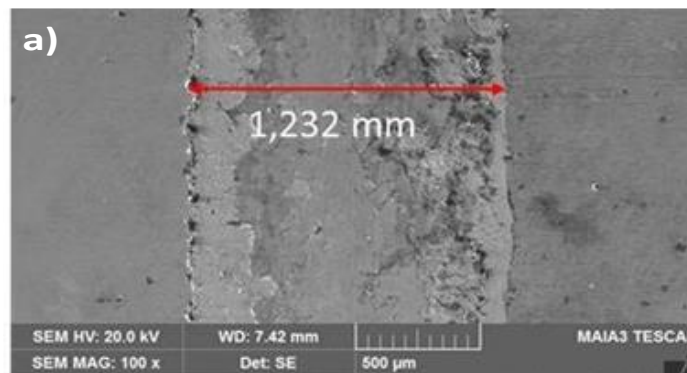


Fig. 9 a) Uncoated dry, b) Uncoated distilled water, c) Tungsten carbide (WC) coated dry, d) Tungsten carbide (WC) coated distilled water

SEM images obtained for the analysis of wear mechanisms are given in Figure 10. In Figure 10, it is seen that the wear trace widths of the coated and uncoated samples at the level of mm in dry environment decreased to the level of μm in the pure water environment. Thanks to the tribofilm layer formed by the water, the contact points between the abrasive ball and the steel material have decreased. The reduced contact between materials limited the width of the wear scar.

In the SEM image of the uncoated sample given in Figure 10.a, it is seen that an aggressive abrasive wear mechanism has occurred. While a regular friction scar formation was observed in the center of the wear steel, irregular formations were observed in the marginal regions of the steel. These irregular formations can be explained by the adhesive effect and the ploughing effect created by the particles detached from the central region. It can be argued that more than one wear mechanism is effective due to excessive entropy in a dry friction environment, but the wear is predominantly abrasive due to stable boundaries in the material. In Figure 10.b, it is seen that a more superficial abrasive wear mechanism is formed by the liquid film effect compared to the dry environment (Figure 10.a). In the images of the WC coated sample given in Figure 10.c and Figure 10.d, it is seen that flaking mechanisms occur on the surface. Spalling wear is a mechanism frequently observed in steel material due to fatigue.

The capillary cracks, which are formed by the effect of tangential and radial forces on the steel surface, expand due to the cyclic load and are effective in the formation of the flaking mechanism. However, it is seen that the flaking in Figure 10.c is more superficial than the flaking images in the literature. Since the increase in hardness caused by the effect of tungsten carbide (WC) coating makes the plastic deformation of the material more difficult, flaking has decreased. This shows that the service life of tungsten carbide (WC) coated H13 steel will increase. According to the image given in Figure 10.d, it is seen that the flaking defect increases in the tungsten carbide (WC) coated steel sample under pure water. Although the width of the wear scar was reduced by the liquid effect, flaking became evident due to the formation of a semi-liquid film layer. Excessive pressure at the points where the film layer is torn has caused weld formation and therefore the surface color tone has darkened. The tangential forces acting on the micron-sized weld points ruptured the weld, causing wider flaking layers to form. Depending on this situation, it can be claimed that the tungsten carbide (WC) coated surfaces will deform more in the water environment due to the semi-liquid film layer.



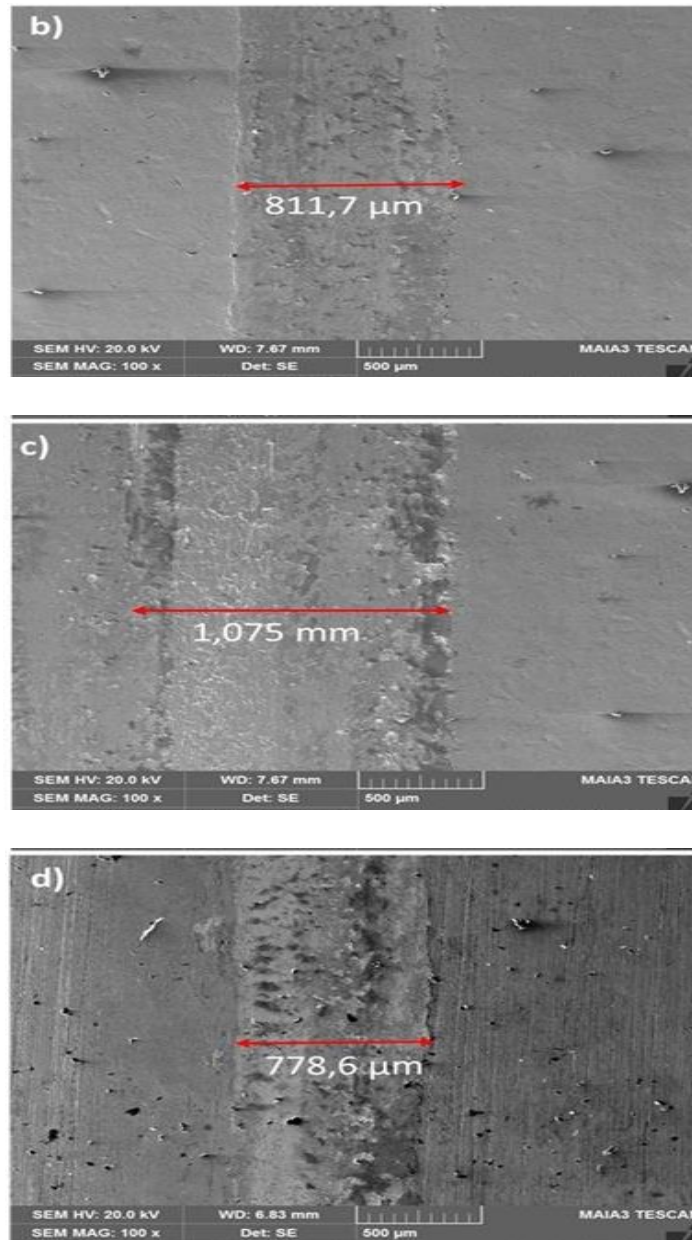


Fig.10 a) uncoated dry, b) Uncoated distilled water, c) Tungsten carbide (WC) coated dry, d) Tungsten carbide (WC) coated distilled water

Topography images obtained from the erosion zones are given in Figure 11. Topography images, coefficient of friction, volume loss, and SEM images were taken into account to validate the results. Ra and Sa values given in Figure 11 show compatibility with other analysis parameters. The fact that Ra and Sa were obtained in numerically small values ($< 0.4 \mu\text{m}$) indicates that abrasive mechanism weighted deformation occurred between the abrasive ball and the H13 steel material. In Figure 11, the red regions represent the peak points, the blue regions the bottom points, and the yellow and green regions represent the minimum surface roughness.

The morphology of Figure 11.a shows that the H13 steel undergoes intense deformation under shear friction. The red regions confirm the existence of the alleged adhesion and ploughing mechanisms according to the SEM images. Again, the aggressive abrasion image determined by SEM images stands out in the midline of the figure. The morphology of the uncoated H13 steel under pure water shows the presence of abrasive wear mechanism in planar form (Figure 11.b). In Figure 11.c, it is seen that a rough surface form is formed due to dry wear conditions. According to the SEM images, the claimed flaking mechanisms could not be clearly seen in the 3D topography images. However, the scarcity of red and blue tones indicates that tungsten carbide (WC) coating increases wear resistance and reduces material loss. In Figure 11.d, it is seen that there is minimal deformation on the surface of the tungsten carbide (WC) coated steel under pure water condition. Thanks to the hardness of the coating and the liquid film layer, the surface appears planar with green and yellow tones. It can be claimed that the ripple formed on the surface is due to the discontinuity of the liquid film layer. The adhesion problem caused by friction in the areas where the liquid film was cut and the high temperature caused micron-level fluctuations on the surface.

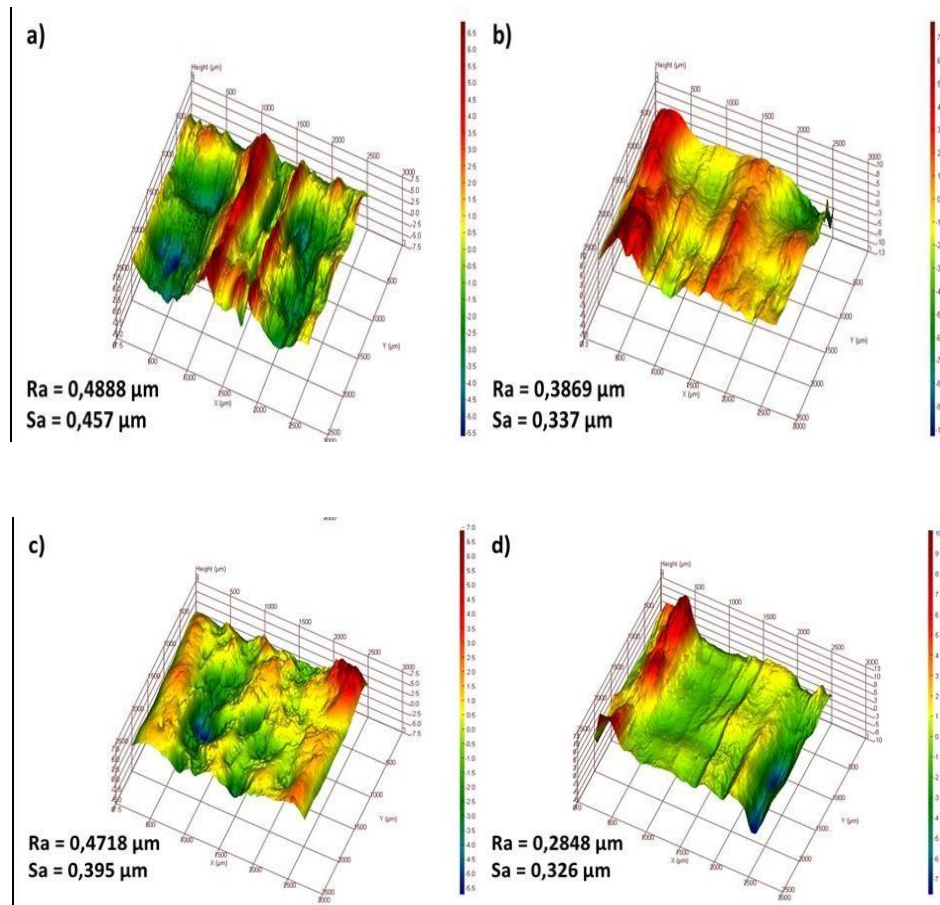


Fig.11 a) uncoated dry, b) Uncoated distilled water, c) Tungsten carbide (WC) coated dry, d) Tungsten carbide (WC) coated distilled water

4. Conclusion

In this study, the effect of WC-Co coating on the wear resistance of H13 steels was investigated. Coating characterization was carried out by analysis of SEM, EDX, XRD images and hardness measurements. For the analysis of the wear test results of the coated and uncoated samples, the friction coefficient and 2D profilometer, SEM and 3D topography images were examined. The results obtained are given below:

- When the SEM images obtained from the coating surfaces were examined, it was determined that the coating thickness was $\sim 165\mu\text{m}$ and that there were minimal gaps and crack defects on the surface. According to the EDX images, the dominant elements were determined as C, W and Co, and it was concluded that the elements were homogeneously distributed according to the elemental mapping images.
- According to the results of the XRD analysis performed to determine the coating surface and the phases in it, it was determined that Fe₃W₃C alloy was formed as a result of the solid state solution formed with the matrix material, and the WC and W₂C phases were intense. According to the microhardness measurement results, it was concluded that the hardness values in the regions where WC and W₂C phases were formed were ~ 750 HV and ~ 1250 HV, respectively.
- According to the friction coefficient results obtained from the wear tests carried out in dry and pure water conditions, it was determined that the friction coefficient of the uncoated sample in pure water environment was 23% lower than in dry environment. This situation is associated with the reduction of compressive and shear stresses of the liquid film layer. It was determined that the friction coefficient (0.023) of the uncoated sample in the pure water environment and the friction coefficient (0.023) of the coated sample in the dry environment were equal. This is explained by the fact that the hardness that increases with the coating layer creates the effect of pure water.
- According to the results obtained from the 2D profilometer images of the samples subjected to the wear test, it was observed that there was a significant wear pit on the uncoated sample surfaces compared to the coated samples. In addition, it was determined that the wear scar depth in the coated samples progressed to a maximum depth of $15\mu\text{m}$, and this was explained by the presence of the high hardness W₂C layer.
- According to the SEM images obtained after the wear tests, it was determined that the width of the wear scar was mm in dry conditions and μm in pure water conditions.
- It has been observed that a more superficial abrasive wear mechanism occurs in pure water conditions compared to dry conditions. It was concluded that the flaking mechanism occurred in the coated samples, but due to the increase in hardness, a more superficial wear mechanism occurred compared to the uncoated samples.
- According to the 3D topography images obtained from the wear surfaces, it was determined that the red and blue color tones were high due to the high roughness in the uncoated samples, and the yellow and green color tones were intense due to the reduced deformation in the coated samples. The results obtained from the 3D topography images are in agreement with the results obtained from the SEM images.

5. References

- [1]. Federici, M., Menapace, C., Moscatelli, A., Gialanella, S., and Straffelini, G., "Effect of Roughness on the Wear Behavior of HVOF Coatings Dry Sliding Against a Friction Material", *Wear*, 368–369: 326–334 (2016).
- [2]. Mishra, T. K., Kumar, A., and Sinha, S. K., "Experimental Investigation and Study of HVOF Sprayed WC-12Co, WC-10Co-4Cr and Cr₃C₂-25NiCr Coating on Its Sliding Wear Behaviour", *International Journal Of Refractory Metals And Hard Materials*, 94: 1–15 (2021).
- [3]. Schubert, J., Houdkova s., Kasparova, M., and cesanek, Z., "Effect of Co Content on the Properties of HVOF Sprayed Coatings Based on Tungsten Carbide", *METAL 2013 - 22nd International Conference On Metallurgy And Materials, Conference Proceedings*, 1100–1105 (2013).
- [4]. Basak, A. K., Celis, J. P., Vardavoulias, M., and Matteazzi, P., "Effect of Nanostructuring and Al Alloying on Friction and Wear Behaviour of Thermal Sprayed WC-Co Coatings", *Surface And Coatings Technology*, 206 (16): 3508– 3516 (2012).
- [5]. Rajinikanth, V. and Venkateswarlu, K., "An Investigation of Sliding Wear Behaviour of WC-Co Coating", *Tribology International*, 44 (12): 1711–1719 (2011).
- [6]. Sahraoui, T., Guessasma, S., Ali Jeridane, M., and Hadji, M., "HVOF Sprayed WC-Co Coatings: Microstructure, Mechanical Properties and Friction Moment Prediction", *Materials And Design*, 31 (3): 1431–1437 (2010).
- [7]. Vashishtha, N., Khatirkar, R. K., and Sapate, S. G., "Tribological behaviour of HVOF sprayed WC-12Co, WC-10Co-4Cr and Cr₃C₂-25NiCr coatings", *Tribology International*, 105 (June 2016): 55–68 (2017).
- [8]. Mateen, A., Saha, G. C., Khan, T. I., and Khalid, F. A., "Tribological behaviour of HVOF sprayed near-nanostructured and microstructured WC-17wt.%Co coatings", *Surface And Coatings Technology*, 206 (6): 1077–1084 (2011).
- [9]. Jalali Azizpour, M. and Tolouei-Rad, M., "The Effect of Spraying Temperature on the Corrosion and Wear Behavior of HVOF Thermal Sprayed WC-Co Coatings", *Ceramics International*, 45 (11): 13934–13941 (2019).
- [10]. Kuçuk, Y., Erdogan, A., "Investigation of high temperature dry sliding behavior of borided H13 hot work tool steel with nanoboron powder", *Surface and Coatings Technology*, 357 (September 2018): 886–895 (2019).
- [11]. Zeng, D., Lu, L., Zhang, N., Gong, Y., and Zhang, J., "Effect of different strengthening methods on rolling/sliding wear of ferrite-pearlite steel", *Wear*, 358–359: 62–71 (2016).
- [12]. Cetin, M. H. and Korkmaz, S., "Investigation of the concentration rate and aggregation behaviour of nano-silver added colloidal suspensions on wear behaviour of metallic materials by using ANOVA method", *Tribology International*, 147 (January): 106273 (2020).
- [13]. Kondul, B., and Cetin, M. H., "Investigation of Wear Behavior of Boronized H13 Steel under Environment of Nano-Silver-Added Lubricants Coated with Different Ligands", *Surface Topography: Metrology and Properties*, 8 (1): (2020).
- [14]. Ma, L., He, C. G., Zhao, X. J., Guo, J., Zhu, Y., Wang, W. J., Liu, Q. Y., and Jin, X. S., "Study on wear and rolling contact fatigue behaviors of wheel/rail materials under different slip ratio conditions", *Wear*, 366–367: 13–26 (2016).
- [15]. Dokumaci, E., Ozkan, I., and Anay, B., "Effect of boronizing on the cyclic oxidation of stainless steel", *Surface and Coatings Technology*, 232: 22–25 (2013).
- [16]. Olugbade, T.O. and Lu, J., "Literature Review on the Mechanical Properties of Materials After Surface Mechanical Attrition Treatment (SMAT)", *Nano Materials Science*, 2:3-31 (2020)
- [17]. Pan, Q. and Lu, L., "Improved Fatigue Resistance of Gradient Nanograined Metallic Materials: Suppress Strain Localization and Damage Accumulation", *Scripta Materialia*, 187:301-306 (2020)

- [18]. Estrin, Y. and Vinogradov, A., "Extreme Grain Refinement by Severe Plastic Deformation: A Wealth of Challenging Science", Sciverse Sciencedirect, 61:782-817 (2013).
- [19]. Cheng, X., Jiang, Z., Wei, D., Hao, L., Wu, H., Xia, W., Zhang, X., Luo, S., and Jiang, L., "Effects of surface preparation on tribological behaviour of a ferritic stainless steel in hot rolling", Wear, 376-377: 1804-1813 (2017).
- [20]. Mateen, A., Saha, G. C., Khan, T. I., and Khalid, F. A., "Tribological behaviour of HVOF sprayed near-nanostructured and microstructured WC-17wt.%Co coatings", Surface And Coatings Technology, 206 (6): 1077-1084 (2011).
- [21]. Ma, G., Wang, L., Gao, H., Zhang, J., and Reddyhoff, T., "The friction coefficient evolution of a TiN coated contact during sliding wear", Applied Surface Science, 345: 109-115 (2015).
- [22]. Amin, S. and Panchal, H., "A review on thermal spray coating processes", International Journal Of Current Trends In Engineering & Research, 2 (4): 556-563 (2016).
- [23]. Vashishtha, N., Khatirkar, R. K., and Sapate, S. G., "Tribological behaviour of HVOF sprayed WC-12Co, WC-10Co-4Cr and Cr₃C₂-25NiCr coatings", Tribology International, 105 (June 2016): 55-68 (2017).
- [24]. Yang, Y., Yao, W., and Zhang, H., "Phase constituents and mechanical properties of laser in-situ synthesized TiCN/TiN composite coating on Ti-6Al-4V", Surface And Coatings Technology, 205 (2): 620-624 (2010).